



1 **Characterization of water-soluble brown carbon chromophores**
2 **from wildfire plumes in the western US using size exclusion**
3 **chromatography**

4 Lisa Azzarello¹, Rebecca A. Washenfelder², Michael A. Robinson^{2,3}, Alessandro Franchin^{2,3,4},
5 Caroline C. Womack^{2,3}, Christopher D. Holmes⁵ Steven S. Brown^{2,6}, Ann Middlebrook², Tim
6 Newberger⁷, Colm Sweeney⁷, Cora J. Young¹

7 ¹Department of Chemistry, York University, Toronto, ON, M3J 1P3, Canada

8 ²Chemical Sciences Laboratory, National Oceanic and Atmospheric Administration, 325
9 Broadway, Boulder, CO 80305, USA

10 ³Cooperative Institute for Research in Environmental Sciences (CIRES), University of Colorado,
11 Boulder, CO, 80309, USA

12 ⁴Now at: National Center for Atmospheric Research, Boulder, CO, USA

13 ⁵Earth, Ocean, and Atmospheric Science, Florida State University, Tallahassee, FL 32304, USA

14 ⁶Department of Chemistry, University of Colorado Boulder, Boulder, Colorado, USA

15 ⁷Global Monitoring Laboratory, National Oceanic and Atmospheric Administration, 325
16 Broadway, Boulder, CO 80305, USA

Correspondence to: C. J. Young (youngcj@yorku.ca)



17 **Abstract**

18 Wildfires are an important source of carbonaceous aerosol in the atmosphere. Organic
19 aerosol that absorbs light in the ultraviolet to visible spectral range is referred to as “brown carbon”
20 (BrC), and its impact on Earth’s radiative budget has not been well characterized. We collected
21 water-soluble brown carbon using a particle into liquid sampler (PILS) onboard a Twin Otter
22 aircraft during the Fire Influence on Regional to Global Environments and Air Quality (FIREX-
23 AQ) campaign. Samples were collected downwind of wildfires in the western United States from
24 August to September 2019. We applied size exclusion chromatography (SEC) with ultraviolet-
25 visible spectroscopy to characterize the molecular size distribution of BrC chromophores. The
26 wildfire plumes had transport ages of 0 to 5 h and the absorption was dominated by chromophores
27 with molecular weights <500 Da. With BrC normalized to a conserved biomass burning tracer,
28 carbon monoxide, a consistent decrease in BrC absorption with plume age was not observed during
29 FIREX-AQ. These findings are consistent with the variable trends in BrC absorption with plume
30 age reported in recent studies. While BrC absorption trends were broadly consistent between the
31 offline SEC analysis and the online PILS measurements, the absolute values of absorption and
32 their spectral dependence differed. We attribute this difference to the organic modifier used in the
33 chromatographic separation and demonstrate how this affects the molecular structure of the
34 compounds comprising BrC, with implications for interpretation of absorption measurement of
35 BrC field samples.



36 **1. Introduction**

37 The wildfire season across the western United States has greatly intensified over the past
38 century. The U.S. Forest Service reports that the amount of western U.S. land burned by “high
39 severity” wildfires (i.e., fires that destroy more than 95% of vegetation) has increased eightfold
40 since 1985 (Parks and Abatzoglou, 2020). A variety of factors influence the number and intensity
41 of wildfires, including fuel availability, temperature, drought conditions, location of lightning
42 strikes, and direct human influence. During the 20th century, fire suppression tactics were applied
43 throughout the western U.S. and these efforts caused fuel to accumulate (Marlon et al., 2012). The
44 combination of dry conditions, warmer temperatures, and fuel availability contributes to the
45 intensity of present-day wildfires in the western U.S. Consequently, the impact that these climatic
46 conditions have on wildfire activity has been established. However, feedback effects that wildfires
47 have on climate is an ongoing area of research.

48 Wildfires emit carbonaceous particulate matter into the atmosphere (Bond et al., 2004; van
49 der Werf et al., 2010). Based on volatility and optical properties, carbonaceous aerosol particles
50 emitted from biomass burning are categorized as elemental carbon (EC) and organic carbon (OC)
51 (Turpin et al., 1990). Elemental carbon, referred to as black carbon (BC), is refractory and is
52 characterized by broad absorbance across the ultraviolet (UV) to infrared wavelengths (Seinfeld
53 and Pankow, 2003; Andreae and Gelencsér, 2006; Laskin et al., 2015). The light-absorbing
54 components of organic aerosols are referred to as brown carbon (BrC) (Laskin et al., 2015). The
55 direct absorption and scattering of solar radiation by these aerosol particles impacts the global
56 radiative budget (Boucher, O.; Randall, D.; Artaxo, P.; Bretherton, C.; Feingold et al., 2013;
57 Forster, P.; Ramaswamy, V.; Artaxo, P.; Berntsen, T.; Betts et al., 2007), but there is uncertainty
58 about the magnitude of this effect. Currently, more information is known about BC and its impact
59 on climate than BrC, as BrC is more chemically complex and more reactive (Buis, 2021; Di
60 Lorenzo et al., 2017). The direct radiative forcing of BC has been estimated to be the second largest
61 anthropogenic climate forcing species (Ramanathan and Carmichael, 2008) and studies have
62 suggested that BrC can contribute between 20 to 40 % to positive radiative forcing from total
63 carbonaceous absorbing aerosol (Feng et al., 2013; Zhang et al., 2017; Zeng et al., 2020a).

64 Wildfire emissions are a dominant primary source of BrC (Washenfelder et al., 2015). The
65 brown colour results from a combination of species with varying abilities to absorb light in the



66 UV-visible region (from highly to weakly absorbing) (Hems et al., 2021). The pyrolysis of lignin
67 and cellulose contributes to the major chemical constituents in wildfire plumes, such as phenolic
68 compounds and organic acids (Simoneit, 2002; Xie et al., 2019; Smith et al., 2014). Lignin
69 pyrolysis products with aromatic functionalities absorb visible light and may contribute to the
70 absorption properties of BrC (Hems et al., 2021). Secondary processes also contribute to BrC
71 formation. The generation of secondary organic aerosol (SOA) stemming from gas phase reaction
72 products includes nitration of aromatic compounds in the presence of NO_x or NO₃ (Harrison et al.,
73 2005; Finewax et al., 2018; Xie et al., 2017). For example, catechol can react with either the NO₃
74 or OH radical to form 4-nitrocatechol (Finewax et al., 2018) and oxidation of toluene under
75 elevated NO_x conditions has been observed to form over 15 absorbing compounds with
76 nitroaromatics contributing up to 60% of absorption in the visible region (Liu et al., 2016).
77 Although there are hypotheses about the identity of BrC chromophores, up to 40% of BrC
78 constituents remain unidentified (Lin et al., 2017; Bluvshstein et al., 2017).

79 To characterize the absorbing constituents that contribute to BrC absorption, reverse phase
80 high performance liquid chromatography (HPLC) coupled to high resolution mass spectrometry
81 has been applied (Fleming et al., 2020). However, fresh and aged BrC consist of extremely low
82 volatile organic compounds (ELVOCs) that may be irreversibly retained on a traditional C₁₈
83 reverse phase HPLC column (Di Lorenzo and Young, 2016). Size exclusion chromatography
84 coupled to ultraviolet-visible absorption spectroscopy (SEC-UV) has been demonstrated as an
85 alternative that successfully measures the absorption properties of high and low molecular weight
86 (MW) ELVOCs in fresh and aged biomass burning-derived samples (Di Lorenzo and Young,
87 2016; Di Lorenzo et al., 2017; Wong et al., 2019). Analysis by SEC-UV has been previously
88 applied to samples collected during ground-based field measurement campaigns, where the
89 method has established the quantification of BrC absorbance as a function of MW and provided
90 insight into the composition of BrC. High MW (>400 Da) compounds with unknown structural
91 identities have been determined to contribute to BrC absorption and the relative contribution to
92 BrC absorption by high MW species increases with smoke age (Di Lorenzo et al., 2017; Wong et
93 al., 2017, 2019). These findings suggested that lower MW species are less persistent in biomass
94 burning smoke relative to higher MW species, likely due to volatilization, oxidation,
95 polymerization, or other processes (Di Lorenzo et al., 2017; Hems et al., 2021).



96 The Fire Influence on Regional to Global Environments and Air Quality (FIREX-AQ) field
97 campaign examined the impact of wildfires on atmospheric chemistry and air quality in the western
98 United States. In this work, we present the SEC-UV analysis of water-soluble BrC that was
99 collected on board the National Oceanic and Atmospheric Administration (NOAA) Twin Otter
100 aircraft during plume transects downwind from western U.S forest fires. These represent the first
101 aircraft samples analyzed by SEC-UV to characterize BrC. We compare the total absorption
102 measured in online and offline samples and attribute assign the BrC absorption to different MW
103 classes. Finally, we examine how the composition of the mobile phase used in the SEC-UV
104 analysis impacts elution time and spectral features. This provides cautionary information about
105 interpreting absorption results in studies that apply chromatographic separation in an aqueous-
106 organic matrix.

107

108 **2. Experimental Approach**

109 **2.1 Overview of the FIREX-AQ field campaign**

110 FIREX-AQ was a multi-platform field campaign that investigated wildfire emissions in the
111 western United States from Jul to Sep 2019. Instrumented aircraft and mobile laboratories were
112 used to intercept and sample smoke plumes throughout multiple western U.S. states. These
113 included a DC-8, ER-2, and two Twin Otter aircraft. This study focuses on smoke sampled by the
114 “Chemistry” Twin Otter aircraft, which was based in Boise, Idaho, from 29 Jul to 5 Sep 2019, and
115 briefly in Cedar City, Utah, from 19 Aug to 23 Aug 2019. The Twin Otter payload included gas
116 and aerosol instruments to measure smoke composition, transport, and transformation. This
117 included CO measurements by near infrared cavity ring-down spectroscopy (Picarro G2401m)
118 (Crosson, 2008; Karion et al., 2013). A complete description of the payload installed on the Twin
119 Otter can be found in Warneke et al. (2023). The payload limited the duration of in-flight sampling
120 to 2.5 – 3 h, with a typical schedule of two or three flights per day during the afternoon, evening,
121 or night. A total of 40 flights were completed in Arizona, Idaho, Nevada, Oregon, and Utah.
122 Airmass back trajectory analyses were used to estimate the plume age of each transect, as described
123 in Liao et al. (2021) and Washenfelder et al. (2022). Briefly, the smoke age was calculated by
124 summing the horizontal advection and vertical plume rise ages between the time of emission and
125 the aircraft interception of the smoke plume. For the Twin Otter flights, many plume intercepts by
126 the aircraft were approximately Lagrangian (Washenfelder et al., 2022).



127 **2.2 Online measurement of water-soluble absorption and offline sample collection**

128 The Brown Carbon-Particle into Liquid Sampler (BrC-PILS) collected online absorption
129 data and offline aqueous samples for the SEC-UV analysis. A complete description of the BrC-
130 PILS instrument and sampling can be found in Zeng et al. (2021) and Washenfelder et al. (2022).
131 Briefly, the BrC-PILS sampled smoke through a shared aerosol inlet on the Twin Otter. A parallel-
132 plate carbon filter denuder removed volatile organic compounds prior to the aerosol entering the
133 PILS. The PILS consisted of a steam generator and droplet impactor to collect aerosols into
134 aqueous solution. The liquid flow then entered a liquid waveguide capillary cell (LWCC) to
135 measure absorption. The instrument precision (3σ) for absorption at 365 nm was $\pm 0.02 \text{ Mm}^{-1}$ for
136 10 s in-flight data, with an uncertainty of $\pm 11\%$ (Zeng et al., 2021). The flow exiting the LWCC
137 was split between a total organic carbon (TOC) analyzer and an automated 14-port valve. The
138 valve directed aqueous sample flow to one of 12 polypropylene sample tubes for offline SEC-UV
139 analysis (Figure S1). Prior to deployment, each polypropylene tube was rinsed with 18.2 M Ω ·cm
140 water (Thermo Scientific Barnstead Smart2Pure) eight to ten times. The sample flow rate was
141 monitored by a liquid mass flow meter prior to the flow diverting between the automated valve
142 and the TOC analyzer. The sample flow was 1.53 mL min⁻¹ during inflight sampling, and the
143 excess 0.43 mL min⁻¹ was collected into an individual polypropylene tube for 12 s to 10 min.
144 During in-flight sampling, the flight scientist actively controlled the sample collection into each
145 polypropylene tube to target transects of the smoke plume (example shown in Figure S2). Six to
146 twelve aqueous samples were collected for each flight, with 201 total samples from 39 science
147 flights. Field blanks of the 18.2 M Ω ·cm water (DIW) used to operate the BrC-PILS were stored
148 similarly in clean polypropylene sample tubes at the beginning, halfway point, and end of
149 campaign. Once collected in the field, the samples and blanks were stored on ice for several hours
150 prior to refrigeration until analysis.

151

152 **2.3 Offline Analysis by SEC-UV**

153 Measurement by SEC-UV provides information about size-dependent light absorption
154 properties of BrC chromophores. The offline aerosol samples were separated using an aqueous
155 gel-filtration column with a MW range of 250 Da to 75 kDa (Polysep GFC P-3000, Phenomenex,
156 Torrence, CA). Size-resolved components were detected using a diode array detector from 190 to
157 800 nm (UltiMate 3000, Thermo Scientific, Sunnyvale, CA) coupled to an ion chromatograph



158 (ICS 6000; Thermo Scientific) pump with an AS autosampler (Thermo Scientific). The isocratic
159 method was run using a 1:1 mixture of acetonitrile and a buffer solution consisting of 18.2 M Ω ·cm
160 deionized water with 25 mM ammonium acetate at a flow rate of 1 mL min⁻¹ and a sample injection
161 volume of 100 μ L. Discussion of the SEC-UV method development and details of the conversion
162 of SEC-UV signal to ambient absorption in units of Mm⁻¹ can be found in the SI. We calculated
163 BrC absorption as a function of MW by applying the calibration method described by Di Lorenzo
164 and Young (2016) (Figure S3). Sample measurements were blank subtracted. The detection limit
165 of the total integrated absorption (equivalent to 3 σ of n=6 field blanks) was 2.5 \pm 0.2 mAU \times min
166 and 0.70 \pm 0.02 mAU \times min at 250 nm and 300 nm, respectively. This corresponds to approximately
167 525 Mm⁻¹ at 250 nm and 150 Mm⁻¹ at 300 nm.

168

169 **3. Results and discussion**

170 **3.1. Trends in absorption with plume age**

171 We present molecular size-resolved absorption for flights that met the following criteria:
172 (1) maximum CO concentrations greater than 0.2 ppmv; (2) three or more downwind plume
173 transects; (3) three or more aqueous samples collected; and (4) consistent wind direction. Of the
174 201 aqueous samples collected, 47 samples from six flights met the criteria and are summarized
175 in Table S1. Each aqueous sample had a measurable absorption signal in the deep UV region (250
176 to 300 nm), while the absorption signal above 300 nm was nearly indistinguishable from the
177 blanks, because the samples were relatively dilute. The average integrated absorption of the 47
178 samples that met the criteria was 10.4 \pm 4.9 mAU \times min (8134 \pm 3857 Mm⁻¹) and 0.36 \pm 0.28
179 mAU \times min (316 \pm 214 Mm⁻¹) for 250 and 300 nm, respectively.

180 To account for plume dilution, we follow the convention of normalizing BrC absorption to
181 a conserved tracer, to calculate $\Delta\text{Abs}_{\lambda, \text{BrC}}/\Delta\text{CO}$ (Forrister et al., 2015; Di Lorenzo et al., 2017;
182 Washenfelder et al., 2022; Zeng et al., 2021), where ΔCO is the average CO mixing ratio measured
183 during each aqueous sample collection subtracted from the average CO background outside the
184 plume. Background BrC absorption at 365 nm (a common wavelength to report BrC absorption)
185 was less than 0.2 Mm⁻¹ and no background correction was made to determine $\Delta\text{Abs}_{\lambda, \text{BrC}}$
186 (Washenfelder et al., 2022). Figure 1 shows $\Delta\text{Abs}_{300\text{nm}, \text{BrC}}/\Delta\text{CO}$ as a function of plume age for the
187 six selected flights, with a linear fit to each flight. The fitted slopes for $\Delta\text{Abs}_{300\text{nm}, \text{BrC}}/\Delta\text{CO}$ vs
188 plume age vary from -0.21 to 0.88 Mm⁻¹ ppbv⁻¹ h⁻¹, and show different trends between flights. This



189 indicates that BrC absorption increased downwind in some plumes and decreased downwind in
190 others. Previous studies of normalized BrC absorption with plume age have reported conflicting
191 results. In the earliest aircraft study, Forrister et al. (2015) collected filter samples from two fires
192 in the western U.S. and measured the BrC absorption from water and methanol extracts. They
193 observed that BrC absorption at 365 nm decayed exponentially over a plume age range spanning
194 0 to 50 h (Figure S6) (Forrister et al., 2015). Di Lorenzo et al. (2017) reported total absorption of
195 size-resolved BrC chromophores using SEC-UV from three locations that were influenced to
196 varying degrees by biomass burning smoke, and observed minimal $\Delta\text{Abs}_{\lambda, \text{BrC}}/\Delta\text{CO}$ change as a
197 function of transport times from 10 to >72 h (Figure S6). In contrast to these measurements of
198 relatively aged biomass burning aerosol, two studies from other FIREX-AQ instruments showed
199 different trends for relatively fresh plumes. Using BrC-PILS measurements from the Twin Otter,
200 Washenfelder et al. (2022) showed variable trends in $\Delta\text{Abs}_{365\text{nm}, \text{BrC}}/\Delta\text{CO}$ slope values ranging
201 from -0.02 to $0.02 \text{ Mm}^{-1} \text{ ppbv}^{-1} \text{ h}^{-1}$ over 0 to 5 h. Using filter samples from the DC-8 aircraft, Zeng
202 et al. (2022) showed that BrC increased, decreased, or was unchanged as a function of plume age
203 over 0 to 8 h.

204 Our results are consistent with the other published results from the FIREX-AQ campaign
205 and differ from the previous studies that examined longer plume ages. The relatively narrow plume
206 age range of the FIREX-AQ sampling makes it challenging to deduce long-term trends associated
207 with changes in total absorption as a function of transport time. In addition, the disparity in
208 $\Delta\text{Abs}_{\lambda, \text{BrC}}/\Delta\text{CO}$ time dependence between FIREX-AQ observations and those reported by Forrister
209 et al. (2015) may be attributed to i) FIREX-AQ having sampled a greater number of western U.S
210 forest fires and ii) the younger age of the FIREX-AQ plumes. More in-flight sampling would be
211 required to observe BrC absorption of plume ages 5 h to 50 h to determine if the results observed
212 by Forrister et al. (2015) would also show variability with a greater number of fires, or if the BrC
213 lifetime would converge to a similar value.

214 **3.2 Chemical evolution of brown carbon with plume age**

215 Chromophores <500 Da were responsible for most of the absorption at 250-300 nm
216 measured in the aqueous samples (Figure 2, Figure S7). When pooling all 47 samples, molecular
217 species >500 Da contributed an average of 3.0 ± 1.9 % to total measured absorption at 250 nm,
218 while molecular species <500 Da contributed an average of 72 ± 4.5 %. Absorption past the
219 exclusion volume represents an unidentified MW, as elution past this retention time (Figure S3)



220 indicates non-SEC analyte-column interactions were occurring. The average contribution to total
221 measured absorption by undefined MW species was 25.1 ± 5.7 %. Previous SEC-UV analyses have
222 observed elution beyond the exclusion volume and non-size exclusion effects (Wong et al., 2017;
223 Lyu et al., 2021). Elution at later retention times has been observed for fresh BrC separated in a
224 mobile phase also containing 50% acetonitrile (Lyu et al., 2021). This result was attributed to non-
225 size exclusion effects, such as hydrophobic interactions of BrC with the SEC stationary phase,
226 which may also have contributed to elution past the exclusion volume in our samples. The
227 absorption density plots of the aqueous samples from the flights listed in Table S1 had similar size-
228 resolved features with varying magnitude in absorption (Figure S7).

229 These results are the first reported SEC-UV measurements of very fresh (0-5 h) field
230 samples of biomass burning smoke, and they confirm some of the trends from field studies that
231 measured more aged smoke, as well as laboratory studies that generated or aged smoke. Previous
232 studies that examined biomass burning BrC using SEC-UV have concluded that fresh, less aged
233 smoke contains a large fraction of lower MW absorbing species (Di Lorenzo et al., 2017; Wong et
234 al., 2017; Lyu et al., 2021). In the examination of field samples, Di Lorenzo et al. (2017) collected
235 ambient biomass burning aerosols that had been aged 10 to >72 h. They observed that low MW
236 (<500 Da) chromophores contributed more to total absorption than higher MW (>500 Da)
237 compounds in the least aged (10 to 15 h) biomass burning-derived filter extracts (Di Lorenzo et
238 al., 2017). These findings resemble the absorption features of our FIREX-AQ samples, which span
239 a plume age range from 0 to 5 hours. Wong et al. (2019) collected filter extracts collected during
240 fire seasons in Greece that correspond to an atmospheric aging time range of 1 to ~70 h, analyzed
241 with SEC-UV, and observed that high MW species dominated total BrC absorption of the fresh
242 and aged smoke. The FIREX-AQ aqueous samples represent the first water-soluble BrC collected
243 in solution downwind of western U.S wildfires. Differences between the FIREX-AQ aqueous
244 samples and the results presented by Wong et al. (2019) can be driven by varying types of fuel
245 emissions, photochemical conditions, meteorology, and differences in back trajectory analyses.
246 Two studies have applied SEC-UV analysis to lab-generated or lab-aged smoke samples. Wong et
247 al. (2017) pyrolyzed dry hardwood and aged the samples from 0 to 10 h with UV light. They found
248 that low MW chromophores dominated total absorption compared to high MW species, which is
249 generally consistent with our observations. Lyu et al. (2021) generated biomass burning aerosol
250 from laboratory combustion of boreal peat and also analyzed the aerosol by SEC-UV. Under the



251 same SEC-UV separation conditions, the FIREX-AQ water aqueous samples parallel the findings
252 of Lyu et al. (2021), with low MW BrC chromophores dominating total absorption for unaged
253 fresh smoke and smoke aged between 0 to 5 h in the atmosphere.

254 **3.3 Comparison of SEC-UV and BrC-PILS absorption**

255 Online and offline absorption sampling are complimentary. The online sampling by the
256 BrC-PILS provides continuous data with much higher time resolution (reported at 10 s), but it is
257 limited to two measurements: water-soluble absorption as a function of wavelength and water-
258 soluble organic carbon concentration. In contrast, the offline samples can be examined using SEC-
259 UV, C₁₈ chromatography, and other analytical techniques that are not feasible onboard an aircraft.
260 During FIREX-AQ, the BrC-PILS measured online water-soluble absorption in the same aqueous
261 flow that was collected for offline sampling. These are the only samples whose absorption was
262 measured online and then subsequently offline during FIREX-AQ. A comparison of the water-
263 soluble absorption measured by the BrC-PILS, and the SEC-UV analysis are shown in Figure 3.
264 Due to logistical constraints during FIREX-AQ, a reference solution was not routinely run on the
265 BrC-PILS instrument or the SEC-UV method to characterize the total absorption observed by both
266 instruments.

267 We observe two major differences between the online and offline samples. First, the total
268 absorption by the SEC-UV measurements is approximately an order of magnitude greater than the
269 BrC-PILS measurements at 300 nm. Second, the BrC-PILS measured BrC absorption between 310
270 and 500 nm. Although the SEC-UV measured between 190 and 800 nm, no absorption
271 distinguishable from the blanks was observed above 310 nm. The comparison between the offline
272 and online work presented here can be compared to previous non-co-located online-offline
273 intercomparison studies. Di Lorenzo et al. (2017) compared offline absorption measurements by
274 SEC-UV of filter extracts to PILS-LWCC online measurements during the Southern Oxidant and
275 Aerosol Study (SOAS). Although the SEC-UV offline samples and online measurements during
276 SOAS were not co-located, they showed reasonable agreement with moderate correlation. Neither
277 method was consistently higher than the other and the median ratio (SEC-UV offline to PILS-
278 LWCC online) was 0.9 (Figure S8). In that study, discrepancies between the offline and online
279 measurements were attributed to differences in locations and inlet characteristics, as well as the
280 solubilization methods (extraction via sonication in water for offline SEC-UV and collision with
281 impaction plate for online PILS-LWCC) (Di Lorenzo et al., 2017). Differences observed in the



282 FIREX-AQ aqueous samples, and the previous comparison between the online-offline BrC
283 samples indicate the necessity to investigate a potential explanation for these inconsistencies. Since
284 the online BrC-PILS and offline SEC-UV samples represent the same samples, solubilization
285 differences between aerosol collection methods cannot explain the variability observed between
286 our measurements. We examine solvent effects as a potential explanation.

287 **3.4 Solvents affect the measured absorption spectra**

288 Plausible chemical structures of chromophores responsible for BrC absorption have been
289 identified and consist of conjugated systems functionalized with hydroxyls, amines, nitro,
290 carbonyls, and carboxylic acid groups (Laskin et al., 2015; Hems et al., 2021; Lin et al., 2017;
291 Fleming et al., 2020; Zeng et al., 2020b; Hettiyadura et al., 2021; Marrero-Ortiz et al., 2019; De
292 Haan et al., 2018; Ji et al., 2022). To compare the online and offline measurements, an assessment
293 of solvation effects due to changes in the mobile phase were considered. For the online
294 measurements, the PILS solubilizes BrC in pure water to facilitate absorption measurements
295 (Weber et al., 2001). The mobile phase used for the offline SEC-UV analysis was a mixture of a
296 buffer solution and acetonitrile. Chromatographic packing materials are often not compatible with
297 pure water and require a mixture with an organic solvent to elute compounds from the stationary
298 phase, or to prevent disrupt partitioning or adsorption in an SEC column. For this reason,
299 chromatographic partitioning-based separations occur in aqueous-organic mixtures, where the
300 composition can be deliberately modified to optimize interactions of the target molecules between
301 the stationary phase and mobile phase. Organic solvents can impact both molecular structure of
302 BrC chromophores and their absorption properties. Since BrC is comprised of a variety of
303 compounds, each component's ability to be solvated depends on the molecular structure of the
304 BrC constituent and on the solvent (Chen et al., 2022). For instance, methanol is commonly used
305 as a BrC extraction solvent due to its efficiency in extracting oxygenated compounds (Chen and
306 Bond, 2010). Methanol is commonly used as a mobile phase component in liquid chromatographic
307 separations. However, methanol can introduce artifacts and alter molecular structures. For
308 example, methanol can react with carbonyl groups to form new structures such as esters, acetals,
309 and hemiacetals (Walser et al., 2008; Bateman et al., 2008; Chen et al., 2022). The mobile phase
310 solvent used here was acetonitrile, for which reactions with typical BrC components have not been
311 observed and has been recommended as a more inert solvent for extraction and analysis (Walser
312 et al., 2008; Bateman et al., 2008; Chen et al., 2022), yet offers a similar dielectric potential and



313 intermolecular interactions between solvent and solute. Thus, this is unlikely to be the source of
314 the absorption differences observed between the online and offline measurements in our work.

315 To assess whether solvent absorption effects could account for our online and offline
316 differences, a standard solution of 4-nitrocatechol was run on both the BrC-PILS using water only
317 and bypassing the PILS. The solution only passed through the LWCC and spectrophotometer as a
318 result. This 4-nitrocatechol solution was also injected into the diode array detector without the
319 SEC column in water and other mobile phases (Figure 4A). The absorption magnitude and
320 wavelength distribution for 4-nitrocatechol were comparable between the literature absorption
321 spectrum and the offline and online measurements when made in water (Hinrichs et al., 2016).
322 Absorption of 4-nitrocatechol changed when the water-acetonitrile mixture was used as the mobile
323 phase, with the absorption maximum red-shifting by approximately 100 nm. Effects of solvent on
324 molecular absorption are well established in the photochemistry literature (Lignell et al., 2014; Mo
325 et al., 2017; Zheng et al., 2018; Lyu et al., 2021; Chen et al., 2022; Dalton et al., 2023). The polarity
326 of the solvent affects the absorption wavelength by changing stabilization of the ground and/or
327 excited states. Our observation is consistent with decreased solvent polarity of acetonitrile-water
328 (relative to water) leading to decreased stabilization of the ground state of the transition in 4-
329 nitrocatechol. However, this effect is molecule dependent, as another BrC constituent, *o*-cresol,
330 showed similar absorption spectra in both acetonitrile and water (Zheng et al., 2018). A biomass
331 burning-derived sample does not contain only a single compound, but is rather a complex
332 combination of various compounds including aromatic organic acids, nitroaromatics, flavonoids,
333 and polycyclic aromatic hydrocarbons (Lin et al., 2018; Fleming et al., 2020), each of which will
334 have unique solvent absorption effects. We examined the effects of solvent on absorption of the
335 complex environmental mixture Suwanee River Fulvic Acid (SRFA II; International Humic
336 Substances Society, Saint Paul, MN, USA), which is a reference material that contains a mixture
337 of molecules with absorption properties comparable to BrC (Figure 4B). As expected, we observed
338 differences in absorption intensity and wavelength in the different solvents. Notably, we observed
339 that absorption in acetonitrile-water was blue-shifted and changed in intensity relative to
340 absorption in water. The intensity in acetonitrile-water was higher at shorter wavelengths and
341 lower at longer wavelengths. If the BrC in our samples was subject to similar effects, this could
342 explain some or all of the differences we observed between online and offline measurements,
343 namely the reduced absorption at longer wavelengths and greater absorption at shorter



344 wavelengths in the offline SEC-UV analysis. This demonstrates that careful consideration of
345 potential solvent effects is required in any comparison of online and offline measurements,
346 particularly between datasets.

347

348 **4. Conclusions and implications**

349 During FIREX-AQ, instruments onboard the NOAA Twin Otter aircraft sampled smoke
350 plumes from wildfires in the western United States with plume ages of 0 to 5 h. The BrC-PILS
351 measured water-soluble BrC absorption online and collected aerosol in aqueous solution for offline
352 SEC-UV analysis. The aqueous samples were collected during downwind plume transects and the
353 online data was collected continuously during inflight sampling. SEC-UV analysis shows that BrC
354 absorption was dominated by chromophores <500 Da. This finding is consistent with reports of
355 laboratory-generated fresh smoke samples. Integrated absorption at 300 nm from the SEC-UV
356 analysis was used to calculate trends in normalized BrC absorption as a function of plume age.
357 These trends were variable and did not show an exponential decay, which is consistent with
358 recently published results from the FIREX-AQ field campaign that examined normalized BrC
359 absorption trends for plumes over 0 to 10 h. Comparison of the online and offline analyses of the
360 same aqueous extracts reveals discrepancies, specifically higher absorption intensity and
361 absorption at lower wavelengths. These discrepancies between online and offline samples
362 demonstrate the importance of solvent effects, which were demonstrated through absorption
363 measurements under different solvent conditions. This highlights the importance of careful
364 consideration of potential solvent effects when comparing online and offline measurements of BrC
365 and when assessing BrC solubility. Offline absorption measurement conditions can alter the
366 molecular structural of BrC constituents and impact the wavelength dependence of the absorption.
367

368 **Acknowledgements**

369 We thank Carsten Warneke, Joshua Schwarz, James Crawford, and Jack Dibb for organizing the
370 FIREX-AQ field campaign. We thank the NOAA Aircraft Operations Center for support during
371 the field mission. L.A. was supported by a Mitacs Globalink Research Internship and an NSERC
372 Discovery Grant. The FIREX-AQ project was supported by the NOAA Atmospheric Chemistry,
373 Carbon, and Climate Program (AC4). We thank Robert Di Lorenzo and Trevor VandenBoer for
374 helpful discussions.



375 **Data Availability Statement**

376 The data used in the study are publicly available at <https://www-air.larc.nasa.gov/missions/firex->

377 [aq/](#)

378 **Competing Interests**

379 At least one of the (co-)authors is a member of the editorial board of Atmospheric Chemistry and
380 Physics.



381 **References**

- 382 Andreae, M. O. and Gelencsér, A.: Black carbon or brown carbon? The nature of light-absorbing
383 carbonaceous aerosols, *Atmospheric Chemistry & Physics*, 6, 3131–3148,
384 <https://doi.org/10.5194/acp-6-3131-2006>, 2006.
- 385 Bateman, A. P., Walser, M. L., Desyaterik, Y., Laskin, J., Laskin, A., and Nizkorodov, S. A.:
386 The effect of solvent on the analysis of secondary organic aerosol using electrospray ionization
387 mass spectrometry., *Environ Sci Technol*, 42, 7341–7346, <https://doi.org/10.1021/es801226w>,
388 2008.
- 389 Bluvshstein, N., Lin, P., Flores, M., Segev, L., Mazar, Y., Tas, E., Snider, G., Weagle, C., Brown,
390 S., Laskin, A., and Rudich, Y.: Broadband optical properties of biomass burning aerosol and
391 identification of brown carbon chromophores, *Journal of Geophysical Research: Atmospheres*,
392 122, 5441–5456, <https://doi.org/10.1002/2016JD026230>, 2017.
- 393 Bond, T. C., Streets, D. G., Yarber, K. F., Nelson, S. M., Woo, J.-H., and Klimont, Z.: A
394 technology-based global inventory of black and organic carbon emissions from combustion,
395 *Journal of Geophysical Research: Atmospheres*, 109, <https://doi.org/10.1029/2003JD003697>,
396 2004.
- 397 Boucher, O.; Randall, D.; Artaxo, P.; Bretherton, C.; Feingold, G. ; Forster, P.; Kerminen, V.
398 M.; Kondo, Y.; Liao, H.; Lohmann, U. ; and Rasch, P.; Satheesh, S. K.; Sherwood, S.; Stevens,
399 B.; Zhang, X. Y.: Clouds and Aerosols. In: *Climate Change 2013: The Physical Science Basis.*
400 *Contribution of Working Group I to the Fifth Assessment Report of the Intergovernmental Panel*
401 *on Climate Change*, in: *Climate Change 2013: The Physical Science Basis. Contribution of*
402 *Working Group I to the Fifth Assessment Report of the Intergovernmental Panel on Climate*
403 *Change*, Cambridge University Press:, New York, NY, 2013.
- 404 Buis, A.: The Climate Connections of a Record Fire Year in the U.S. West – Climate Change:
405 Vital Signs of the Planet: [https://climate.nasa.gov/blog/3066/the-climate-connections-of-a-](https://climate.nasa.gov/blog/3066/the-climate-connections-of-a-record-fire-year-in-the-us-west/)
406 [record-fire-year-in-the-us-west/](https://climate.nasa.gov/blog/3066/the-climate-connections-of-a-record-fire-year-in-the-us-west/), 2021.
- 407 Chen, K., Raeofy, N., Lum, M., Mayorga, R., Woods, M., Bahreini, R., Zhang, H., and Lin, Y.-
408 H.: Solvent effects on chemical composition and optical properties of extracted secondary brown



- 409 carbon constituents, *Aerosol Science and Technology*, 56, 917–930,
410 <https://doi.org/10.1080/02786826.2022.2100734>, 2022.
- 411 Chen, Y. and Bond, T. C.: Light absorption by organic carbon from wood combustion,
412 *Atmospheric Chemistry and Physics*, 10, 1773–1787, <https://doi.org/10.5194/acp-10-1773-2010>,
413 2010.
- 414 Crosson, E. R.: A cavity ring-down analyzer for measuring atmospheric levels of methane,
415 carbon dioxide, and water vapor, *Applied Physics B*, 92, 403–408,
416 <https://doi.org/10.1007/s00340-008-3135-y>, 2008.
- 417 Dalton, A. B., Le, S. M., Karimova, N. V., Gerber, R. B., and Nizkorodov, S. A.: Influence of
418 solvent on the electronic structure and the photochemistry of nitrophenols, *Environ. Sci.: Atmos.*,
419 3, 257–267, <https://doi.org/10.1039/D2EA00144F>, 2023.
- 420 De Haan, D. O., Tapavicza, E., Riva, M., Cui, T., Surratt, J. D., Smith, A. C., Jordan, M.-C.,
421 Nilakantan, S., Almodovar, M., Stewart, T. N., de Loera, A., De Haan, A. C., Cazaunau, M.,
422 Gratien, A., Pangui, E., and Doussin, J.-F.: Nitrogen-containing, light-absorbing oligomers
423 produced in aerosol particles exposed to methylglyoxal, photolysis, and cloud cycling, *Environ.*
424 *Sci. Technol.*, 52, 4061–4071, <https://doi.org/10.1021/acs.est.7b06105>, 2018.
- 425 Di Lorenzo, R. A. and Young, C. J.: Size separation method for absorption characterization in
426 brown carbon: Application to an aged biomass burning sample, *Geophysical Research Letters*,
427 43, 458–465, <https://doi.org/10.1002/2015GL066954>, 2016.
- 428 Di Lorenzo, R. A., Washenfelder, R. A., Attwood, A. R., Guo, H., Xu, L., Ng, N. L., Weber, R.
429 J., Baumann, K., Edgerton, E., and Young, C. J.: Molecular-size-separated brown carbon
430 absorption for biomass-burning aerosol at multiple field sites, *Environmental Science and*
431 *Technology*, 51, 3128–3137, <https://doi.org/10.1021/acs.est.6b06160>, 2017.
- 432 Feng, Y., Ramanathan, V., and Kotamarthi, V. R.: Brown carbon: a significant atmospheric
433 absorber of solar radiation?, *Atmospheric Chemistry and Physics*, 13, 8607–8621,
434 <https://doi.org/10.5194/acp-13-8607-2013>, 2013.
- 435 Finewax, Z., de Gouw, J. A., and Ziemann, P. J.: Identification and quantification of 4-
436 nitrocatechol formed from OH and NO₃ radical-initiated reactions of catechol in air in the



- 437 presence of NO_x: implications for secondary organic aerosol formation from biomass burning,
438 *Environ. Sci. Technol.*, 52, 1981–1989, <https://doi.org/10.1021/acs.est.7b05864>, 2018.
- 439 Fleming, L. T., Lin, P., Roberts, J. M., Selimovic, V., Yokelson, R., Laskin, J., Laskin, A., and
440 Nizkorodov, S. A.: Molecular composition and photochemical lifetimes of brown carbon
441 chromophores in biomass burning organic aerosol, *Atmospheric Chemistry and Physics*, 20,
442 1105–1129, <https://doi.org/10.5194/acp-20-1105-2020>, 2020.
- 443 Forrister, H., Liu, J., Scheuer, E., Dibb, J., Ziemba, L., Thornhill, K. L., Anderson, B., Diskin,
444 G., Perring, A. E., Schwarz, J. P., Campuzano-Jost, P., Day, D. A., Palm, B. B., Jimenez, J. L.,
445 Nenes, A., and Weber, R. J.: Evolution of brown carbon in wildfire plumes, *Geophysical*
446 *Research Letters*, 42, 4623–4630, <https://doi.org/10.1002/2015GL063897>, 2015.
- 447 Forster, P.; Ramaswamy, V.; Artaxo, P.; Berntsen, T.; Betts, R. ; Fahey, D. W.; Haywood, J.;
448 Lean, J.; Lowe, D. C.; Myhre, G. ; N., and J.; Prinn, R.; Raga, G.; Schulz, M.; Van Dorland, R.:
449 In *Climate Change 2007: The Physical Science Basis. Contribution of Working Group I to the*
450 *Fourth Assessment Report of the Intergovernmental Panel on Climate Change*, Cambridge
451 University Press: Cambridge, United Kingdom and New York, NY, 2007; pp 129–243, 2007.
- 452 Harrison, M. A. J., Barra, S., Borghesi, D., Vione, D., Arsene, C., and Iulian Olariu, R.: Nitrated
453 phenols in the atmosphere: a review, *Atmospheric Environment*, 39, 231–248,
454 <https://doi.org/10.1016/j.atmosenv.2004.09.044>, 2005.
- 455 Hems, R. F., Schnitzler, E. G., Liu-Kang, C., Cappa, C. D., and Abbatt, J. P. D.: Aging of
456 atmospheric brown carbon aerosol, *ACS Earth and Space Chemistry*, 5, 722–748,
457 <https://doi.org/10.1021/acsearthspacechem.0c00346>, 2021.
- 458 Hettiyadura, A. P. S., Garcia, V., Li, C., West, C. P., Tomlin, J., He, Q., Rudich, Y., and Laskin,
459 A.: Chemical composition and molecular-specific optical properties of atmospheric brown
460 carbon associated with biomass burning., *Environ Sci Technol*, 55, 2511–2521,
461 <https://doi.org/10.1021/acs.est.0c05883>, 2021.
- 462 Hinrichs, R. Z., Buczek, P., and Trivedi, J. J.: Solar absorption by aerosol-bound nitrophenols
463 compared to aqueous and gaseous nitrophenols., *Environ Sci Technol*, 50, 5661–5667,
464 <https://doi.org/10.1021/acs.est.6b00302>, 2016.



- 465 Ji, Y., Shi, Q., Ma, X., Gao, L., Wang, J., Li, Y., Gao, Y., Li, G., Zhang, R., and An, T.:
466 Elucidating the critical oligomeric steps in secondary organic aerosol and brown carbon
467 formation, *Atmospheric Chemistry and Physics*, 22, 7259–7271, [https://doi.org/10.5194/acp-22-](https://doi.org/10.5194/acp-22-7259-2022)
468 7259-2022, 2022.
- 469 Karion, A., Sweeney, C., Wolter, S., Newberger, T., Chen, H., Andrews, A., Kofler, J., Neff, D.,
470 and Tans, P.: Long-term greenhouse gas measurements from aircraft, *Atmospheric Measurement*
471 *Techniques*, 6, 511–526, <https://doi.org/10.5194/amt-6-511-2013>, 2013.
- 472 Laskin, A., Laskin, J., and Nizkorodov, S. A.: Chemistry of Atmospheric Brown Carbon,
473 *Chemical Reviews*, 115, 4335–4382, <https://doi.org/10.1021/cr5006167>, 2015.
- 474 Liao, J., Wolfe, G. M., Hannun, R. A., St. Clair, J. M., Hanisco, T. F., Gilman, J. B., Lamplugh,
475 A., Selimovic, V., Diskin, G. S., Nowak, J. B., Halliday, H. S., DiGangi, J. P., Hall, S. R.,
476 Ullmann, K., Holmes, C. D., Fite, C. H., Agastra, A., Ryerson, T. B., Peischl, J., Bourgeois, I.,
477 Warneke, C., Coggon, M. M., Gkatzelis, G. I., Sekimoto, K., Fried, A., Richter, D., Weibring, P.,
478 Apel, E. C., Hornbrook, R. S., Brown, S. S., Womack, C. C., Robinson, M. A., Washenfelder, R.
479 A., Veres, P. R., and Neuman, J. A.: Formaldehyde evolution in US wildfire plumes during the
480 Fire Influence on Regional to Global Environments and Air Quality experiment (FIREX-AQ),
481 *Atmospheric Chemistry and Physics*, 21, 18319–18331, [https://doi.org/10.5194/acp-21-18319-](https://doi.org/10.5194/acp-21-18319-2021)
482 2021, 2021.
- 483 Lignell, H., Hinks, M. L., and Nizkorodov, S. A.: Exploring matrix effects on photochemistry of
484 organic aerosols, *Proceedings of the National Academy of Sciences*, 111, 13780–13785,
485 <https://doi.org/10.1073/pnas.1322106111>, 2014.
- 486 Lin, P., Bluvshstein, N., Rudich, Y., Nizkorodov, S. A., Laskin, J., and Laskin, A.: Molecular
487 chemistry of atmospheric brown carbon inferred from a nationwide biomass burning event,
488 *Environmental Science & Technology*, 51, 11561–11570,
489 <https://doi.org/10.1021/acs.est.7b02276>, 2017.
- 490 Lin, P., Fleming, L. T., Nizkorodov, S. A., Laskin, J., and Laskin, A.: Comprehensive molecular
491 characterization of atmospheric brown carbon by high resolution mass spectrometry with
492 electrospray and atmospheric pressure photoionization., *Anal Chem*, 90, 12493–12502,
493 <https://doi.org/10.1021/acs.analchem.8b02177>, 2018.



- 494 Liu, J., Lin, P., Laskin, A., Laskin, J., Kathmann, S. M., Wise, M., Caylor, R., Imholt, F.,
495 Selimovic, V., and Shilling, J. E.: Optical properties and aging of light-absorbing secondary
496 organic aerosol, *Atmospheric Chemistry and Physics*, 16, 12815–12827,
497 <https://doi.org/10.5194/acp-16-12815-2016>, 2016.
- 498 Lyu, M., Thompson, D. K., Zhang, N., Cuss, C. W., Young, C. J., and Styler, S. A.: Unraveling
499 the complexity of atmospheric brown carbon produced by smoldering boreal peat using size-
500 exclusion chromatography with selective mobile phases, *Environ. Sci.: Atmos.*, 1, 241–252,
501 <https://doi.org/10.1039/D1EA00011J>, 2021.
- 502 Marlon, J. R., Bartlein, P. J., Gavin, D. G., Long, C. J., Anderson, R. S., Briles, C. E., Brown, K.
503 J., Colombaroli, D., Hallett, D. J., Power, M. J., Scharf, E. A., and Walsh, M. K.: Long-term
504 perspective on wildfires in the western USA, *Proceedings of the National Academy of Sciences*,
505 109, E535 LP-E543, <https://doi.org/10.1073/pnas.1112839109>, 2012.
- 506 Marrero-Ortiz, W., Hu, M., Du, Z., Ji, Y., Wang, Y., Guo, S., Lin, Y., Gomez-Hernandez, M.,
507 Peng, J., Li, Y., Secretst, J., Zamora, M. L., Wang, Y., An, T., and Zhang, R.: Formation and
508 optical properties of brown carbon from small α -dicarbonyls and amines, *Environ. Sci. Technol.*,
509 53, 117–126, <https://doi.org/10.1021/acs.est.8b03995>, 2019.
- 510 Mo, Y., Li, J., Liu, J., Zhong, G., Cheng, Z., Tian, C., Chen, Y., and Zhang, G.: The influence of
511 solvent and pH on determination of the light absorption properties of water-soluble brown
512 carbon, *Atmospheric Environment*, 161, 90–98, <https://doi.org/10.1016/j.atmosenv.2017.04.037>,
513 2017.
- 514 Parks, S. A. and Abatzoglou, J. T.: Warmer and Drier Fire Seasons Contribute to Increases in
515 Area Burned at High Severity in Western US Forests From 1985 to 2017, *Geophysical Research*
516 *Letters*, 47, e2020GL089858, <https://doi.org/10.1029/2020GL089858>, 2020.
- 517 Ramanathan, V. and Carmichael, G.: Global and regional climate changes due to black carbon,
518 *Nat Geosci*, 1, <https://doi.org/10.1038/ngeo156>, 2008.
- 519 Seinfeld, J. H. and Pankow, J. F.: Organic Atmospheric Particulate Material, *Annual Review of*
520 *Physical Chemistry*, 54, 121–140, <https://doi.org/10.1146/annurev.physchem.54.011002.103756>,
521 2003.



- 522 Simoneit, B. R. T.: Biomass burning — a review of organic tracers for smoke from incomplete
523 combustion, *Applied Geochemistry*, 17, 129–162, <https://doi.org/10.1016/S0883->
524 2927(01)00061-0, 2002.
- 525 Smith, J. D., Sio, V., Yu, L., Zhang, Q., and Anastasio, C.: Secondary organic aerosol production
526 from aqueous reactions of atmospheric phenols with an organic triplet excited state,
527 *Environmental Science & Technology*, 48, 1049–1057, <https://doi.org/10.1021/es4045715>, 2014.
- 528 Turpin, B. J., Cary, R. A., and Huntzicker, J. J.: An in situ, time-resolved analyzer for aerosol
529 organic and elemental carbon, *Aerosol Science and Technology*, 12, 161–171,
530 <https://doi.org/10.1080/02786829008959336>, 1990.
- 531 Walser, M. L., Desyaterik, Y., Laskin, J., Laskin, A., and Nizkorodov, S. A.: High-resolution
532 mass spectrometric analysis of secondary organic aerosol produced by ozonation of limonene,
533 *Phys. Chem. Chem. Phys.*, 10, 1009–1022, <https://doi.org/10.1039/B712620D>, 2008.
- 534 Warneke, C., Schwarz, J. P., Dibb, J., Kalashnikova, O., Frost, G., Al-Saad, J., Brown, S. S.,
535 Brewer, Wm. A., Soja, A., Seidel, F. C., Washenfelder, R. A., Wiggins, E. B., Moore, R. H.,
536 Anderson, B. E., Jordan, C., Yacovitch, T. I., Herndon, S. C., Liu, S., Kuwayama, T., Jaffe, D.,
537 Johnston, N., Selimovic, V., Yokelson, R., Giles, D. M., Holben, B. N., Goloub, P., Popovici, I.,
538 Trainer, M., Kumar, A., Pierce, R. B., Fahey, D., Roberts, J., Gargulinski, E. M., Peterson, D. A.,
539 Ye, X., Thapa, L. H., Saide, P. E., Fite, C. H., Holmes, C. D., Wang, S., Coggon, M. M., Decker,
540 Z. C. J., Stockwell, C. E., Xu, L., Gkatzelis, G., Aikin, K., Lefer, B., Kaspari, J., Griffin, D.,
541 Zeng, L., Weber, R., Hastings, M., Chai, J., Wolfe, G. M., Hanisco, T. F., Liao, J., Campuzano
542 Jost, P., Guo, H., Jimenez, J. L., Crawford, J., and The FIREX-AQ Science Team: Fire Influence
543 on Regional to Global Environments and Air Quality (FIREX-AQ), *Journal of Geophysical*
544 *Research: Atmospheres*, 128, e2022JD037758, <https://doi.org/10.1029/2022JD037758>, 2023.
- 545 Washenfelder, R., Attwood, A., Brock, C., Guo, H., Xu, L., Weber, R., Ng, N., Allen, H., Ayres,
546 B., Baumann, K., Cohen, R., Draper, D., Duffey, K., Edgerton, E., Fry, J., Hu, W., Jimenez, J.,
547 Palm, B., Romer, P., and Brown, S.: Biomass burning dominates brown carbon absorption in the
548 rural southeastern United States, *Geophysical Research Letters*, 42, 653–664,
549 <https://doi.org/10.1002/2014GL062444>, 2015.



- 550 Washenfelder, R. A., Azzarello, L., Ball, K., Brown, S. S., Decker, Z. C. J., Franchin, A.,
551 Fredrickson, C. D., Hayden, K., Holmes, C. D., Middlebrook, A. M., Palm, B. B., Pierce, R. B.,
552 Price, D. J., Roberts, J. M., Robinson, M. A., Thornton, J. A., Womack, C. C., and Young, C. J.:
553 Complexity in the evolution, composition, and spectroscopy of brown carbon in aircraft
554 measurements of wildfire plumes, *Geophysical Research Letters*, 49, e2022GL098951,
555 <https://doi.org/10.1029/2022GL098951>, 2022.
- 556 Weber, R. J., Orsini, D., Daun, Y., Lee, Y.-N., Klotz, P. J., and Brechtel, F.: A particle-into-
557 liquid collector for rapid measurement of aerosol bulk chemical composition, *Aerosol Science*
558 *and Technology*, 35, 718–727, <https://doi.org/10.1080/02786820152546761>, 2001.
- 559 van der Werf, G. R., Randerson, J. T., Giglio, L., Collatz, G. J., Mu, M., Kasibhatla, P. S.,
560 Morton, D. C., DeFries, R. S., Jin, Y., and van Leeuwen, T. T.: Global fire emissions and the
561 contribution of deforestation, savanna, forest, agricultural, and peat fires (1997–2009),
562 *Atmospheric Chemistry and Physics*, 10, 11707–11735, [https://doi.org/10.5194/acp-10-11707-](https://doi.org/10.5194/acp-10-11707-2010)
563 2010, 2010.
- 564 Wong, J. P. S., Nenes, A., and Weber, R. J.: Changes in light absorptivity of molecular weight
565 separated brown carbon due to photolytic aging, *Environmental Science & Technology*, 51,
566 8414–8421, <https://doi.org/10.1021/acs.est.7b01739>, 2017.
- 567 Wong, J. P. S., Tsagkaraki, M., Tsiodra, I., Mihalopoulos, N., Violaki, K., Kanakidou, M.,
568 Sciare, J., Nenes, A., and Weber, R. J.: Atmospheric evolution of molecular-weight-separated
569 brown carbon from biomass burning, *Atmospheric Chemistry and Physics*, 19, 7319–7334,
570 <https://doi.org/10.5194/acp-19-7319-2019>, 2019.
- 571 Xie, M., Chen, X., Hays, M. D., Lewandowski, M., Offenberg, J., Kleindienst, T. E., and Holder,
572 A. L.: Light Absorption of secondary organic aerosol: composition and contribution of
573 nitroaromatic compounds., *Environ Sci Technol*, 51, 11607–11616,
574 <https://doi.org/10.1021/acs.est.7b03263>, 2017.
- 575 Xie, M., Chen, X., Hays, M. D., and Holder, A. L.: Composition and light absorption of N-
576 containing aromatic compounds in organic aerosols from laboratory biomass burning,
577 *Atmospheric chemistry and physics*, 19, 2899–2915, <https://doi.org/10.5194/acp-19-2899-2019>,
578 2019.



- 579 Zeng, L., Zhang, A., Wang, Y., Wagner, N. L., Katich, J. M., Schwarz, J. P., Schill, G. P., Brock,
580 C., Froyd, K. D., Murphy, D. M., Williamson, C. J., Kupc, A., Scheuer, E., Dibb, J., and Weber,
581 R. J.: Global Measurements of Brown Carbon and Estimated Direct Radiative Effects., *Geophys*
582 *Res Lett*, 47, e2020GL088747, <https://doi.org/10.1029/2020GL088747>, 2020a.
- 583 Zeng, L., Sullivan, A. P., Washenfelder, R. A., Dibb, J., Scheuer, E., Campos, T. L., Katich, J.
584 M., Levin, E., Robinson, M. A., and Weber, R. J.: Assessment of online water-soluble brown
585 carbon measuring systems for aircraft sampling, *Atmospheric Measurement Techniques*, 14,
586 6357–6378, <https://doi.org/10.5194/amt-14-6357-2021>, 2021.
- 587 Zeng, L., Dibb, J., Scheuer, E., Katich, J. M., Schwarz, J. P., Bourgeois, I., Peischl, J., Ryerson,
588 T., Warneke, C., Perring, A. E., Diskin, G. S., DiGangi, J. P., Nowak, J. B., Moore, R. H.,
589 Wiggins, E. B., Pagonis, D., Guo, H., Campuzano-Jost, P., Jimenez, J. L., Xu, L., and Weber, R.
590 J.: Characteristics and evolution of brown carbon in western United States wildfires,
591 *Atmospheric Chemistry and Physics*, 22, 8009–8036, <https://doi.org/10.5194/acp-22-8009-2022>,
592 2022.
- 593 Zeng, Y., Shen, Z., Takahama, S., Zhang, L., Zhang, T., Lei, Y., Zhang, Q., Xu, H., Ning, Y.,
594 Huang, Y., Cao, J., and Rudolf, H.: Molecular absorption and evolution mechanisms of PM_{2.5}
595 brown carbon revealed by electrospray ionization fourier transform–ion cyclotron resonance
596 mass spectrometry during a severe winter pollution episode in Xi’an, China, *Geophysical*
597 *Research Letters*, 47, e2020GL087977, <https://doi.org/10.1029/2020GL087977>, 2020b.
- 598 Zhang, Y., Forrister, H., Liu, J., Dibb, J., Anderson, B., Schwarz, J. P., Perring, A. E., Jimenez, J.
599 L., Campuzano-Jost, P., Wang, Y., Nenes, A., and Weber, R. J.: Top-of-atmosphere radiative
600 forcing affected by brown carbon in the upper troposphere, *Nature Geoscience*, 10, 486–489,
601 <https://doi.org/10.1038/ngeo2960>, 2017.
- 602 Zheng, D., Yuan, X.-A., Ma, H., Li, X., Wang, X., Liu, Z., and Ma, J.: Unexpected solvent
603 effects on the UV/Vis absorption spectra of o-cresol in toluene and benzene: in contrast with
604 non-aromatic solvents, *Royal Society Open Science*, 5, 171928,
605 <https://doi.org/10.1098/rsos.171928>, 2018.



606 **Figure 1.** Absorption at 300 nm to CO as a function of plume age for aqueous samples collected
607 for 6 flights during FIREX-AQ 2019. Absorption measured by SEC-UV with a mobile phase that
608 consisted of equal parts acetonitrile and 18.2 MΩ·cm deionized water with 25 mM ammonium
609 acetate at a flow rate of 1 mL min⁻¹.

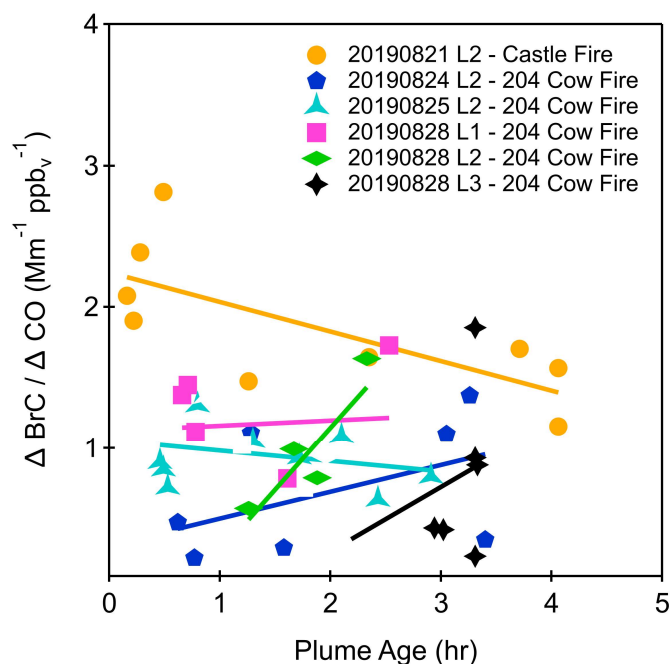
610 **Figure 2.** Absorption contribution of high (>500 Da), low (<500 Da), and unidentified molecular
611 weight species of aqueous collected during the second flight leg on 21 Aug 2019.

612 **Figure 3.** Total absorption measured offline by the SEC-UV (at 300 nm) analysis compared to the
613 total absorption measured online by the BrC-PILS (averaged 310-320 nm). Each colour represents
614 a different flight leg and each marker represents the total absorption measured in each aqueous
615 sample subjected to the SEC-UV analysis. The online absorption measurement was averaged over
616 the time each aqueous sample was collected.

617 **Figure 4.** (a) Absorption cross section of 4-nitrocatechol measured in solution measured using the
618 BrC-PILS (bypassing the PILS), the SEC-UV set-up bypassing the SEC column with two different
619 mobile phases, and by Hinrichs et al. (b) Absorption of fulvic acid measured with the SEC-UV
620 set-up bypassing the column in three different mobile phases.

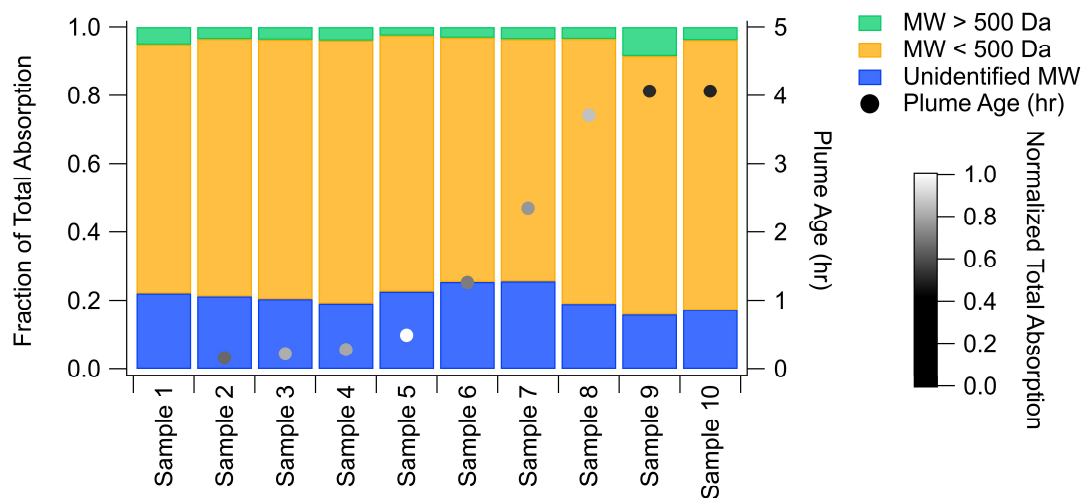


Figure 1.



621
622
623

Figure 2.





624

625 **Figure 3.**

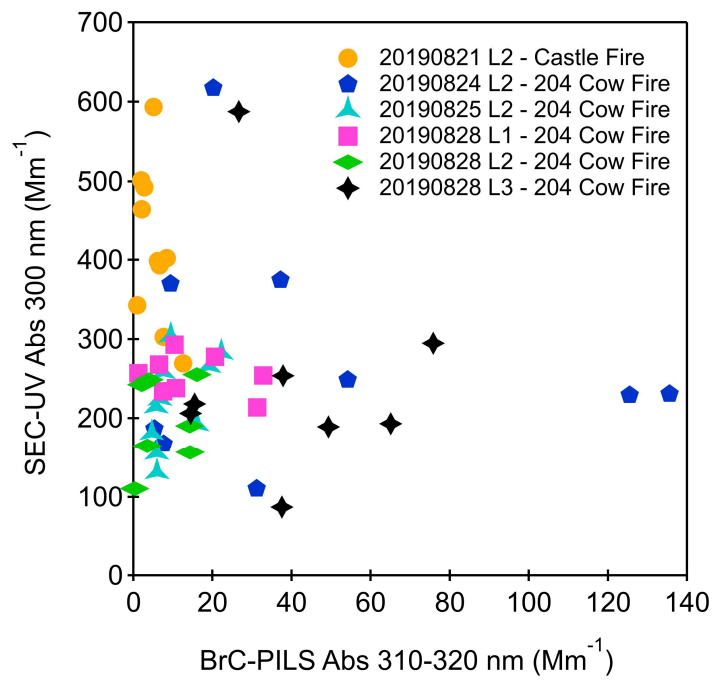




Figure 4.

